

# Low-Cost Robust Distributed Collaborative Beamforming Against Implementation Impairments

Oussama Ben Smida<sup>†</sup>, Slim Zaidi<sup>†\*</sup>, Sofiène Affes<sup>†</sup>, and Shahrokh Valaee<sup>\*</sup>

<sup>†</sup>INRS-EMT, Université du Québec, Montreal, QC, H5A 1K6, Canada, Email: {oussama.ben.smida,affes}@emt.inrs.ca,

<sup>\*</sup>ECE Department, University of Toronto, Toronto, Ontario, M5S 3G4, Canada, Email: {slim.zaidi, valaee}@utoronto.ca

**Abstract**—We propose a new collaborative beamforming (CB) solution robust against major implementation impairments over dual-hop transmissions from a source to a destination communicating through a wireless sensor network (WSN) of  $K$  nodes. In the first time slot, the source sends its signal to the WSN while, in the second, each node forwards its received signal after multiplying it by a properly selected beamforming weight. The latter aims to minimize the received noise power while maintaining the desired power equal to unity. These weights depend a priori on some channel state information (CSI) parameters. Hence, the latter have to be estimated locally at each node thereby resulting in implementation errors that could severely hinder CB performance. Exploiting an efficient asymptotic approximation at large  $K$ , we develop alternative CB solutions that not only account for estimation errors, but also adapt to different implementation scenarios and wireless propagation environments ranging from monochromatic (i.e., scattering-free) to polychromatic (i.e., P-DCB) ones. Besides, in contrast to existing techniques, our new CB solutions are distributed (i.e., DCB) in that they do not require any information exchange among nodes, thereby dramatically improving both WSN spectral and power efficiencies. Simulation results confirm that the proposed DCB techniques are much more robust against implementations errors than their benchmarks at much lower complexity.

**Index Terms**—Collaborative beamforming (CB), robust, distributed, wireless sensor network (WSN), scattering, channel mismatch, implementation impairments.

## I. INTRODUCTION

CB stands out today as a key technique that offering them tremendous capacity, coverage, and power gains. Using CB,  $K$  autonomous and independent sensor nodes relay the information from a desired source to a target destination through a two-hop communication link by estimating then transmitting weighted replicas of the desired signal in the first and second time slots, respectively. The beamforming weights designed so as to optimize an objective function while satisfying some practical constraints. Due to its numerous merits, CB has gained the attention of the research community. [2] introduced the CB concept and analyzed its performance in WSNs. [4] evaluated the CB's beampattern characteristics while [7] designed techniques that narrow down its mainbeam and minimize its sidelobe effect. [6] proposed CB solutions that improve WSN energy efficiency and reduce its nodes

collaboration time and [8] extended the CB applicability range to scattered environments. The advances made from various CB aspects over the past decades or so are properly reviewed in [9].

Despite its advantages, CB inevitably suffers in practice from implementation impairments. Indeed, the beamforming weights often depend on and, hence, require the estimation of CSI parameters locally at each node. Unfortunately, such a process could result in several estimation errors that may cause severe channel mismatch and, hence, dramatically hinder the CB performance. To overcome this shortcoming, [10]-[13] developed new CB techniques robust against such estimation errors. These techniques could be roughly divided into two categories: worst-case and stochastic. The former are designed to handle the worst-case scenario when errors reach their maximum and, hence, can be extremely inefficient when actually the latter are in most real-world conditions subject to random perturbations and/or unbounded. The former are more robust since their design accounts for random errors. Nevertheless, they have some drawbacks on their own. Indeed, they rely very often on iterative greedy suboptimal search approaches that explore a daunting number of potential solutions. Unfortunately, WSN nodes find their extremely limited computing and power capabilities severely burdened and quickly exhausted or depleted. Besides, their robustness very often deteriorate drastically in the presence of large channel estimation errors and, hence, become unsuitable for hostile wireless environments. More importantly, stochastic CB techniques suffer from another major implementation impairment: the key fact they do not offer distributed solutions. Indeed, the weights depend on each other node information, which are locally unavailable. Although robust to small errors, their implementation requires in real-world operating conditions huge information exchange among all nodes. The required overwhelming data overhead could starve to "death" the very limited computing and power capabilities of WSN nodes, very often found already exhausted and depleted (cf. above), and, if not enough, could dramatically degrade their spectrum efficiency.

We propose a new CB solution robust against major implementation impairments over dual-hop transmissions from a source to a destination communicating through a WSN of  $K$  nodes. Exploiting an efficient asymptotic approximation at large  $K$ , we develop alternative CB solutions that not only account for estimation errors, but also adapt to different

Work supported by the NSERC/Huawei Canada/TELUS CRD Grant on 5G-WAVES (WAV Enabling Schemes), the DG and CREATE PERSWADE <www.create-perswade.ca> Programs of NSERC, and a Discovery Accelerator Supplement Award from NSERC.

implementation scenarios and wireless propagation environments ranging from monochromatic (i.e., scattering-free) to polychromatic (i.e., P-DCB) ones. Besides, in contrast to existing techniques, our new CB solutions are distributed (i.e., DCB) in that they do not require any information exchange among nodes, thereby dramatically improving the WSN spectral and power efficiencies. Simulation results confirm that the proposed DCB techniques are much more robust against implementations errors than their benchmarks at much lower complexity.

The paper is organized as follows. Section II describes the dual-hop communication system model. The proposed robust M-DCB and P-DCB techniques are derived in section III. Section IV analyzes the performance of the proposed techniques in both monochromatic and polychromatic environments. Simulation results are discussed in section V and Section VI draws out concluding remarks.

*Notation* : Uppercase and lowercase bold letters denote matrices and column vectors, respectively.  $[\cdot]_{il}$  and  $[\cdot]_i$  are the  $(i, l)^{th}$  entry of a matrix and  $i^{th}$  entry of a vector, respectively.  $(\cdot)^T$  and  $(\cdot)^H$  denote the transpose and the Hermitian transpose, respectively.  $\|\cdot\|$  is the 2-norm of a vector and  $|\cdot|$  is the absolute value.  $\odot$  is the element-wise product.  $E\{\cdot\}$  stands for the statistical expectation.  $J_1(\cdot)$  is the first-order Bessel function of the first kind.

## II. SYSTEM MODEL

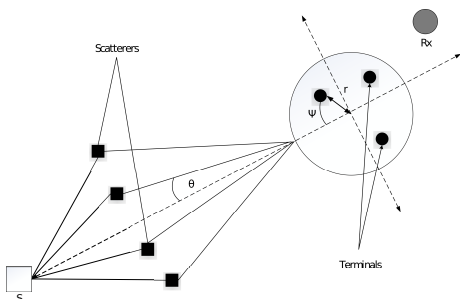


Fig. 1. System model.

As illustrated in Fig. 1, the system of our interest consists of a wireless sensor network (WSN) comprised of  $K$  nodes equipped each with a single isotropic antenna and uniformly and independently distributed on  $D(O, R)$ , the disc with center at  $O$  and radius  $R$ , a receiver  $Rx$ , and a source  $S$  both located in the same plane containing  $D(O, R)$ . We assume that there is no direct link from the source to the receiver due to high pathloss attenuation. Moreover, let  $(A_s, \phi_s)$  denote the source's polar coordinates and  $s$  its narrow-band<sup>1</sup> unit power signal. Without loss of any generality,  $S$  is assumed to be at  $\phi_s = 0$  and to be located far from the nodes, i.e.,  $A_s \gg R$ . Let  $(r_k, \psi_k)$ ,  $[\mathbf{g}]_k$ , and  $[\mathbf{f}]_k$  denote the  $k$ -th node's polar coordinates, backward, and forward channels, respectively.

<sup>1</sup>In this paper, we assume that the signal bandwidth's reciprocal is large with respect to the time delays of all rays. For this reason, the time notion is ignored when denoting the source signal.

$[\mathbf{f}]_k$  is assumed to be a zero-mean unit-variance circular Gaussian random variable. Since WSN nodes are independent and completely autonomous, we consider here that the  $k$ -th WSN is only aware of its coordinates and channels while being oblivious of those of other nodes in the network.

A dual-hop communication is established from the source  $S$  to the receiver  $Rx$ . In the first time slot, the source sends its signal  $s$  to the WSN. Let  $\mathbf{y}$  denotes the received signal vector at the terminals given by

$$\mathbf{y} = \mathbf{g}s + \mathbf{v}, \quad (1)$$

where  $\mathbf{g} \triangleq [[\mathbf{g}]_1 \dots [\mathbf{g}]_K]^T$  and  $\mathbf{v}$  is the nodes' noise vector. In the second time slot, the  $k$ -th node multiplies its received signal with the complex conjugate of the beamforming weight  $w_k$  and forwards the resulting signal to the receiver. It follows from (1) that the received signal at  $O$  is

$$\begin{aligned} r &= \mathbf{f}^T (\mathbf{w}^* \odot \mathbf{y}) + n = \mathbf{w}^H (\mathbf{f} \odot \mathbf{y}) + n \\ &= s \mathbf{w}^H \mathbf{h} + \mathbf{w}^H (\mathbf{f} \odot \mathbf{v}) + n, \end{aligned} \quad (2)$$

where  $\mathbf{w} \triangleq [w_1 \dots w_K]^T$  is the beamforming vector,  $\mathbf{h} \triangleq \mathbf{f} \odot \mathbf{g}$ ,  $\mathbf{f} \triangleq [[\mathbf{f}]_1 \dots [\mathbf{f}]_K]^T$ , and  $n$  is the receiver noise. Let  $P_{\mathbf{w},s}$  and  $P_{\mathbf{w},n}$  denote the received power from the source, and the aggregate noise power due to the thermal noise at the receiver and the forwarded noises from the terminals, respectively. It holds from (2) that

$$P_{\mathbf{w}}(\phi_s) = |\mathbf{w}^H \mathbf{h}|^2 \quad (3)$$

$$P_{\mathbf{w},n} = \sigma_v^2 \mathbf{w}^H \mathbf{\Lambda} \mathbf{w} + \sigma_n^2, \quad (4)$$

where  $\mathbf{\Lambda} \triangleq \text{diag}\{|\mathbf{f}]_1|^2 \dots |\mathbf{f}]_K|^2\}$ . Although several approaches can be adopted to properly design the beamforming weights, we are only concerned in this paper with minimizing the aggregate noise power while maintaining the beamforming response  $\mathbf{w}^H \mathbf{h}$ , and hence, the power received from the source equal to unity. Mathematically, we have to solve the following optimization problem:

$$\mathbf{w}_{\text{opt}} = \arg \min P_{\mathbf{w},n} \quad \text{s.t.} \quad P_{\mathbf{w}}(\phi_s) = 1, \quad (5)$$

where  $\mathbf{w}_{\text{opt}}$  denotes the optimal beamforming vector. The optimization problem in (5) can be rewritten as

$$\mathbf{w}_{\text{opt}} = \arg \max \frac{\mathbf{w}^H \mathbf{h} \mathbf{h}^H \mathbf{w}}{\mathbf{w}^H \mathbf{\Lambda} \mathbf{w}} \quad \text{s.t.} \quad |\mathbf{w}^H \mathbf{h}|^2 = 1. \quad (6)$$

The solution of the above convex optimization problem can be expressed as

$$\mathbf{w}_{\text{opt}} = \frac{\mathbf{\Lambda}^{-1} \mathbf{h}}{|\mathbf{h}^H \mathbf{\Lambda}^{-1} \mathbf{h}|}, \quad (7)$$

and, hence, the  $k$ -th node's weight is given by

$$[\mathbf{w}_{\text{opt}}]_k = \frac{\mathbf{h}_k}{|\mathbf{f}_k| |\mathbf{g}_k|}. \quad (8)$$

It follows from (8) that in order to implement  $\mathbf{w}_{\text{opt}}$ , the  $k$ -th node must estimate both its backward  $[\mathbf{f}]_k$  and forward channels  $[\mathbf{g}]_k$ . Unfortunately, in practice, such a process results in channel estimation errors which may hinder the

beamforming performances. As such,  $\mathbf{w}_{\text{opt}}$  is only valid in ideal conditions where implementation impairments do not exist. In real-world conditions,  $\mathbf{w}_{\text{opt}}$  is substitute by

$$\tilde{\mathbf{w}}_{\text{opt}} = \frac{\tilde{\Lambda}^{-1}\tilde{\mathbf{h}}}{\left|\tilde{\mathbf{h}}^H\tilde{\Lambda}^{-1}\tilde{\mathbf{h}}\right|}, \quad (9)$$

where  $[\tilde{\mathbf{f}}]_k$  and  $[\tilde{\mathbf{g}}]_k$  are the  $k$ -th estimates of the backward and forward channels, respectively. Another drawback of  $\tilde{\mathbf{w}}_{\text{opt}}$  which must be underlined herein is that the  $k$ -th node must be aware of the channel estimates of all other nodes in the WSN. To this end, each node must broadcast its channel information through the network and, hence,  $\tilde{\mathbf{w}}_{\text{opt}}$ 's implementation requires a huge overhead. the latter may cause not only the depletion of the WSN nodes scarce energy resources, but also the deterioration of the WSN spectral efficiency.

In what follows, we propose new CB techniques robust against implementation impairments (i.e., channel estimation errors and high overhead).

### III. PROPOSED ROBUST CB TECHNIQUES

In order to overcome the implementation impairments, one should start by taking an in-depth look into the backward channel structure. Borrowing from the antenna-array literature, two main channel categories exist: i) single-ray (i.e., monochromatic) channels that ignore the scattering phenomenon to assume only a unique line-of-sight ray and ii) multi-ray (i.e., polychromatic) that accounts for the scattering present in most of the real-world environments.

#### A. Monochromatic (i.e., Scattering-Free) Environments

In such environments,  $\mathbf{g}_k$  can be expressed as

$$\mathbf{g}_k = e^{-j\varrho_k}, \quad (10)$$

where  $\varrho_k = \frac{2\pi}{\lambda} r_k \cos(\phi_s - \psi_k)$  is the  $k$ -th node's initial phase. To derive its corresponding beamforming weight, the latter has then two options: estimating from a pilot signal sent from  $S$  either its initial phase  $\varrho_k$  or the direction-of arrival (DoA)  $\phi_s$  and its coordinates  $(r_k, \psi_k)$ . The first option requires the implementation of phase synchronization techniques while the second rely on DoA and localization algorithms. Nevertheless, both options incur estimation errors of different nature that hinder the accuracy of  $\mathbf{g}_k$  and, hence, the performance of CB.

1) *Implementation Option 1: Phase synchronization:* This implementation option results in a phase jitter due to both synchronization and phase offset estimation among nodes. Therefore, the  $k$ -th node's backward channel estimate  $\tilde{\mathbf{g}}_k$  is given

$$\tilde{\mathbf{g}}_k = e^{-j\varrho_k} \Delta_{g_k}, \quad (11)$$

where  $\Delta_{g_k} = e^{-j\delta_k}$  and  $\delta_k$  is the  $k$ -th node's phase jitter that depends on its local oscillator characteristics. We will show later that  $\tilde{\mathbf{w}}_{\text{opt}}$ 's performance deteriorates as  $\delta_k$  increases due to channel mismatch (i.e.,  $\tilde{\mathbf{g}}_k \neq \mathbf{g}_k$ ) it causes. To overcome this challenging issue, we propose in this paper to anticipate the inevitable phase jitter by accounting to this implementation

impairment at the design level. Actually, one could modify the optimization problem in (6) as

$$\mathbf{w}_P = \arg \max \frac{\mathbf{w}^H \tilde{\mathbf{h}} \tilde{\mathbf{h}}^H \mathbf{w}}{\mathbf{w}^H \tilde{\Lambda} \mathbf{w}} \quad \text{s.t.} \quad |\mathbf{w}^H \tilde{\mathbf{h}}|^2 = 1. \quad (12)$$

where  $\tilde{\mathbf{h}}_k = \tilde{\mathbf{f}}_k \tilde{\mathbf{g}}_k$  and  $\tilde{\mathbf{f}}_k = \mathbf{f}_k + \Delta_{f_k}$  with  $\Delta_{f_k}$  the error incurred when estimating the  $k$ -th node backward channel using a training sequence sent from the receiver. The proposed beamforming vector is then given by

$$\mathbf{w}_P = \frac{\tilde{\Lambda}^{-1}\tilde{\mathbf{h}}}{\left|\tilde{\mathbf{h}}^H\tilde{\Lambda}^{-1}\tilde{\mathbf{h}}\right|}. \quad (13)$$

As can be observed from (13),  $\mathbf{w}_P$  depends in both the actual and estimated values of channels. Apparently, this has no sense as nodes are normally unaware of the actual channel information. However, one could substitute  $\tilde{\mathbf{h}}^H\tilde{\Lambda}^{-1}\tilde{\mathbf{h}}$  by an equivalent quantity that depends only on known parameters. To this end, we propose to investigate its asymptotic expression at large  $K$ . Assuming that  $\Delta_{g_k}$  and  $\Delta_{f_k}$  are independent and uniformly distributed over  $[-\sqrt{3}\sigma_g, \sqrt{3}\sigma_g]$  and  $[-\sqrt{3}\sigma_f, \sqrt{3}\sigma_f]$ , respectively, one could obtain

$$\begin{aligned} & \lim_{K \rightarrow +\infty} (\tilde{\mathbf{h}}^H \tilde{\Lambda}^{-1} \tilde{\mathbf{h}})^H (\tilde{\mathbf{h}}^H \tilde{\Lambda}^{-1} \tilde{\mathbf{h}}) = \\ & \mathbb{E} \left\{ \sum_{k=1}^K \sum_{p=1}^K \Delta_{g_k} \Delta_{g_p}^H \right\} + \mathbb{E} \left\{ \sum_{k=1}^K \sum_{p=1}^K \frac{\Delta_{g_k} \mathbf{f}_k^H \Delta_{f_k} \Delta_{g_p}^H \mathbf{f}_p \Delta_{f_p}^H}{|\mathbf{f}_k|^2 |\mathbf{f}_p|^2} \right\} \\ & = K(1 + \sigma_f^2) + K(K-1) \frac{\sin^2(\sqrt{3}\sigma_g)}{3\sigma_g \Delta_g^2}. \end{aligned} \quad (14)$$

where  $\sigma_g$  and  $\sigma_f$  are the variances of  $\Delta_g$  and  $\Delta_f$ , respectively. Please note that in the sixth line, we resort to the law of large numbers and the fact that nodes are uniformly distributed over  $D(O, R)$ . As the number of nodes in WSNs are typically large we can substitute (14) in (13) to finally obtain

$$\mathbf{w}_P \simeq \frac{\tilde{\Lambda}^{-1}\tilde{\mathbf{h}}}{\sqrt{K(1 + \sigma_f^2) + K(K-1) \frac{\sin^2(\sqrt{3}\sigma_g)}{3\sigma_g^2}}}. \quad (15)$$

A straightforward inspection of (15) reveals that  $[\mathbf{w}_P]_k$  is exclusively dependant on  $\tilde{\mathbf{f}}_k$ ,  $\tilde{\mathbf{g}}_k$ ,  $\sigma_g$ , and  $\sigma_f$ . The first and second are locally estimated by the  $k$ -th node while  $\tilde{\mathbf{g}}_k$ ,  $\sigma_g$  depend on its local oscillator characteristics and the adopted phase synchronization technique and, hence, could be stored in its local memory before the WSN deployment. Furthermore,  $[\mathbf{w}_P]_k$  is independent of the forward and backward channels of all other nodes. This is an important feature since it avoids any information exchange among nodes, thereby saving their scarce energy resources and improving the WSN spectral efficiency.

2) *Implementation Option 2: Localization and DoA Estimation:* With option 2, each node must perform both self-localization and DoA estimation algorithm which also usually results in some estimation errors hindering the channel information accuracy. In such a case, the estimated backwards channel can be written as

$$\tilde{\mathbf{g}}_k = e^{-j\frac{2\pi}{\lambda}(r_k + \delta_{r_k}) \cos(\psi_k + \delta_{\psi_k})}. \quad (16)$$

where  $\delta_{r_k}$  is the error on the radial coordinate  $r_k$  and  $\delta_{\psi_k}$  is the combined error on the angle coordinate  $\psi_k$  and the DoA  $\phi_s$  ( $\phi_s = 0$ ). Using similar steps as in Section III-A1, one can prove that the proposed beamforming vector  $\mathbf{w}_P$  can be expressed as

$$\mathbf{w}_P \simeq \frac{\tilde{\mathbf{A}}^{-1} \tilde{\mathbf{h}}}{\sqrt{K(1+\sigma_f^2) + K(K-1) \mathbb{E} \left\{ e^{j \frac{2\pi}{\lambda} (\nu_k - 2R\mu_k \sin(\frac{\delta_{\psi_k}}{2}))} \right\}^2}} \quad (17)$$

where the expectation is taken over  $\nu_k$ ,  $\mu_k$ , and  $\delta_{\psi_k}$ ,  $\nu_k = \delta_{r_k} \cos(\psi_k + \delta_{\psi_k})$ , and  $\mu_k = \frac{r_k}{R} \sin(\psi_k + \frac{\delta_{\psi_k}}{2})$ . As could be observed from (15), using our proposed beamformer, each node is able to compute its own weight using only its local information, thereby avoiding any information exchange that may dramatically deteriorate the network power and spectral efficiencies. However, every node needs to compute the expectation in the RHS of (15), thereby burdening the proposed beamformer's implementation complexity. In what follows, we prove that using mild assumptions, it is possible to derive the latter expectation in closed-form. Assuming that  $\nu_k$  and  $\mu_k$  are statistically independent, we have  $\mathbb{E} \left\{ e^{j \frac{2\pi}{\lambda} (\nu_k - 2R\mu_k \sin(\frac{\delta_{\psi_k}}{2}))} \right\} = \xi_r \xi_{\psi}(0)$  where

$$\xi_r = \mathbb{E}_{\nu_k} \left\{ e^{j \frac{2\pi}{\lambda} \nu_k} \right\}, \quad (18)$$

and

$$\xi_{\psi}(\phi) = \mathbb{E}_{\mu_k, \delta_{\psi_k}} \left\{ e^{-4j\pi R\mu_k \sin(\frac{\phi - \delta_{\psi_k}}{2})} \right\}. \quad (19)$$

The probability density of  $\nu_k$  can be calculated as follows

$$\begin{aligned} f_{\nu_k}(\nu) &= \frac{1}{2\pi\sqrt{3}\sigma_r} \left[ \int_{\nu}^{\sqrt{3}\sigma_r} \frac{1}{\sqrt{\delta_r^2 - \nu^2}} d\delta_r + \int_{-\sqrt{3}\sigma_r}^{-\nu} \frac{1}{\sqrt{\delta_r^2 - \nu^2}} d\delta_r \right], \\ &= \frac{1}{\pi\sqrt{3}\sigma_r} \left( \ln \left( 1 + \sqrt{1 - \frac{\nu^2}{3\sigma_r^2}} \right) - \ln \left( \frac{|\nu|}{\sqrt{3}\sigma_r} \right) \right) \\ &\quad \text{with } |\nu| \leq \sqrt{3}\sigma_r. \end{aligned} \quad (20)$$

Therefore,  $\xi_r$  is given by

$$\begin{aligned} \xi_r &= \int_{-\sqrt{3}\sigma_r}^{\sqrt{3}\sigma_r} \frac{1}{\pi\sqrt{3}\sigma_r} e^{j \frac{2\pi}{\lambda} \nu_k} \left( \ln \left( 1 + \sqrt{1 - \frac{\nu^2}{3\sigma_r^2}} \right) - \ln \left( \frac{|\nu|}{\sqrt{3}\sigma_r} \right) \right) d\nu \\ &= \frac{2}{\pi} \int_0^1 \cos \left( \frac{2\pi}{\lambda} \sqrt{3}\sigma_r t \right) \ln \left( \frac{1 + \sqrt{1 - t^2}}{t} \right) dt \\ &= {}_1F_2 \left( 0.5; 1, 1.5; -3 \left( \frac{\sigma_r}{\lambda} \right)^2 \right). \end{aligned} \quad (21)$$

Please note that in the second line, we resort to a variable change as  $t = \frac{|\nu|}{\sqrt{3}\sigma_r}$ . We also remove the imaginary part of the equation as it is a sinus function, which is odd and, hence, its integral over a zero-centered interval vanishes. On the other hand, we have

$$\begin{aligned} \xi_{\psi}(0) &= \mathbb{E}_{\delta_{\psi_k}} \left\{ \sum_{p=0}^{+\infty} \frac{\left( 4\pi R \sin \left( \frac{-\delta_{\psi_k}}{2} \right) \right)^p}{p!} (-j)^p \mathbb{E}(\mu_k^p) \right\} \\ &= \mathbb{E}_{\delta_{\psi_k}} \left\{ \frac{2J_1 \left( 4\pi R \sin \left( \frac{\delta_{\psi_k}}{2} \right) \right)}{4\pi R \sin \left( \frac{\delta_{\psi_k}}{2} \right)} \right\} \\ &= {}_1F_2 \left( 0.5; 1.5, 2; -3 \left( \frac{R\sigma_{\psi}}{\lambda} \right)^2 \right). \end{aligned} \quad (22)$$

Using (21)-(22) in (17) yields to (23). According to (23),  $w_p$  depends on the coefficients of the estimated channels and  $\sigma_r$ ,  $\sigma_{\psi}$ , and  $\sigma_f$ . The estimated channel coefficients are available at the terminals while  $\sigma_r$ ,  $\sigma_{\psi}$ , and  $\sigma_f$  can be easily distributed over the network at low cost. As each terminal can locally estimate its own channel, its implementation will also reduce overhead and power consumption.

The proposed robust M-DCB is effective in both channel mismatch scenarios. Closed-form solutions enable near-optimal performance with a distributed implementation that reduces the power consumption and the information exchange. In what follows, the scattering effect is not neglected anymore. The transmitted signal generates  $L$  rays, which can induce more ambiguities, and thus more challenges to compute the optimal desired weights.

### B. Polychromatic Environments

We assume here that the source is scattered by a given number of scatterers located in the same plane containing  $D(O, R)$ . The latters generate, from the transmit signal,  $L$  rays or "spatial chromatics" (with reference to their angular distribution) that form a polychromatic propagation channel. The  $l$ -th ray or chromatic is characterized by its angle deviation  $\theta_l$  from the source direction  $\phi_s$  and its complex amplitude  $\alpha_l$ . In such a case, the  $k$ -th node backward channel is given by

$$\mathbf{g}_k = \sum_{l=1}^L \alpha_l e^{-j \frac{2\pi}{\lambda} r_k \cos(\phi_s + \theta_l - \psi_k)}. \quad (24)$$

It is noteworthy that (24) reduces to (10) when there is no scattering (i.e.,  $\theta_l = 0$  and  $\alpha_l = 1/L$ ). It follows from (24) that in polychromatic environments, each node must estimate its polar coordinates  $(r_k, \psi_k)$ , all rays' DoAs  $\phi_s + \theta_l$  and amplitudes  $\alpha_l$ s. This would often result in errors which may cause a channel mismatch, thereby hindering the proposed beamforming performance. The  $k$ -th node backward channel estimate is then given by

$$\tilde{\mathbf{g}}_k = \sum_{l=1}^L \hat{\alpha}_l e^{-j \frac{2\pi}{\lambda} (\hat{r}) \cos(\theta_l - \psi_k + \delta_{\theta_l})}. \quad (25)$$

$$\mathbf{w}_P \simeq \frac{\tilde{\mathbf{\Lambda}}^{-1} \tilde{\mathbf{h}}}{\sqrt{K(1 + \sigma_f^2) + K(K-1) {}_1F_2\left(0.5; 1, 1.5; -3\left(\pi \frac{\sigma_r}{\lambda}\right)^2\right) {}_1F_2\left(0.5; 1.5, 2; -3\left(\pi \frac{R\sigma_\psi}{\lambda}\right)^2\right)^2}}. \quad (23)$$

where  $\tilde{\alpha}_l = \alpha_l + \delta_{\alpha_l}$ ,  $\tilde{r} = r_k + \delta r_k$  and  $\tilde{\theta}_{lk} = \theta_l - \psi_k + \delta \theta_{lk}$  with  $\delta_{\alpha_l}$ ,  $\delta r_k$  and  $\delta \theta_{lk}$  being the estimates of  $l$ -th ray's amplitude, radical coordinate  $r_k$  and phase, respectively. It follows then, from (25), that

$$\begin{aligned} \tilde{\mathbf{h}}^H \tilde{\mathbf{\Lambda}}^{-1} \tilde{\mathbf{h}} &= \sum_{l=1}^L \sum_{m=1}^L \tilde{\alpha}_l^* \alpha_m \sum_{k=1}^K e^{j\beta_{lm} \kappa_{klm}} e^{j\frac{2\pi}{\lambda} \vartheta_{kl}} \\ &+ \sum_{k=1}^K \frac{\tilde{\mathbf{g}}_k^H \mathbf{g}_k \mathbf{f}_k \Delta_{f_k}^H}{|\mathbf{f}_k|^2}. \end{aligned} \quad (26)$$

where  $\kappa_{klm} = r_k \sin\left(\psi_k - \frac{\theta_l + \theta_m + \delta \theta_{lk}}{2}\right)$ ,  $\vartheta_{kl} = \delta r_k \cos(\psi_k - \theta_l - \delta \theta_{lk})$ , and  $\beta_{l,m} = \frac{4\pi R}{\lambda} \sin\left(\frac{\theta_l - \theta_m + \delta \theta_{lk}}{2}\right)$ . Assuming that  $\kappa_{klm}$  and  $\vartheta_{kl}$  are statistically independent, we obtain for large  $K$

$$\begin{aligned} |\tilde{\mathbf{h}}^H \tilde{\mathbf{\Lambda}}^{-1} \tilde{\mathbf{h}}|^2 &\simeq K(K-1) \times \left| \sum_{l=1}^L \sum_{l2=1}^L \hat{\alpha}_l^* \hat{\alpha}_m \frac{2J_1(\beta_{l,m})}{\beta_{l,m}} \right. \\ &\times \left. {}_1F_2\left(0.5; 1, 1.5; -3\left(\frac{\pi\sigma_r}{\lambda}\right)^2\right) \right|^2 + K \sum_{l=1}^L \sum_{m=1}^L \sum_{n=1}^L \hat{\alpha}_l \hat{\alpha}_n^* \\ &\frac{3\sigma_\alpha^2}{L} (A'_{l,m,n,m} + C_{l,m,n}) + K \sum_{l=1}^L \sum_{m=1}^L \sum_{n=1}^L \sum_{o=1}^L \hat{\alpha}_l \hat{\alpha}_m^* \hat{\alpha}_n^* \hat{\alpha}_o \\ &A'_{l,m,n,m} B'_{ln} (1 + \sigma_f^2), \end{aligned} \quad (27)$$

where  $\sigma_r^2$  and  $\sigma_\alpha^2$  are the variances of  $\delta r_k$  and  $\delta_{\alpha_l}$ , respectively.  $A'_{l,m,n,m} = \mathbb{E}_{\kappa} \left\{ e^{j(\beta_{l,m} \kappa_{klm} - \beta_{n,m} \kappa_{knm})} \right\}$ ,  $B'_{ln} = \mathbb{E}_{\vartheta} \left\{ e^{j\frac{2\pi}{\lambda} (\vartheta_{kl} - \vartheta_{kn})} \right\}$  and  $C_{l,m,n} = (K-1) \frac{4J_1(\beta_{l,m})J_1(\beta_{n,m})}{\beta_{l,m}\beta_{n,m}} {}_1F_2\left(0.5; 1, 1.5; -3\left(\frac{\pi\sigma_r}{\lambda}\right)^2\right)$ . Using (27) in (13) yields to the desired beamforming vector  $\mathbf{w}_P$ . As can be observed from  $\mathbf{w}_P$ , in order to compute its corresponding weight, each node requires only its locally available information. Please note that  $\sigma_r$  and  $\sigma_\alpha$  are parameters closely related to the algorithms implemented in the WSN nodes and, hence, may be stored in their local memories before the WSN deployment. Furthermore,  $\mathbf{w}_P$  lends itself to a distributed implementation in WSN even in scattering environments.

#### IV. PERFORMANCE ANALYSIS

In order to verify the efficiency of the proposed beamformer, we analyze in this section the behaviors of its achieved average SNR (ASNR) and compare it to its conventional counterpart. Let  $\gamma_w = \mathbb{E}\{P_w(\phi_s)/P_{w,n}\}$  denote the ASNR achieved by any CB  $\mathbf{w}$  where the expectation is taken over all nodes coordinates, forward and backward channels, and implementation errors. Unfortunately, the derivation of  $\gamma$  in closed-form turns out to be a tedious task if not impossible. In

this work, we propose to study instead another practically appealing metric that is the average signal to average noise ratio (ASANR)  $\bar{\gamma}_w = \bar{P}_w(\phi_s)/\bar{P}_{w,n}$  where  $\bar{P}_w(\phi_s) = \mathbb{E}\{P_w(\phi_s)\}$  and  $\bar{P}_{w,n} = \mathbb{E}\{P_{w,n}\}$ . Please note that [8] has showed that  $\gamma$  and  $\bar{\gamma}$  have approximately the same behaviors. Let us first derive the average received power  $\bar{P}_w(\phi)$  from any source located at  $\phi$  using  $\mathbf{w}$ .

Please note that for the lack of space, we only consider in what follows the monochromatic (i.e., scattering-free) environments where nodes have two implementation options. Beampattern analysis in polychromatic environment will be disclosed in the journal version of this paper.

1) *Implementation Option 1*: Let us first derive the average beampattern achieved by  $\tilde{\mathbf{w}}_{\text{opt}}$ . Exploiting the Taylor series expansion around 0 of the exponential function, we obtain

$$\begin{aligned} \bar{P}_{\tilde{\mathbf{w}}_{\text{opt}}}(\phi) &= \frac{K}{K^2} + \frac{K(K-1)}{K^2} \left[ \sum_{p=0}^{+\infty} \frac{\beta^p(\phi)}{p!} (-j)^p \mathbb{E}(\mu_k^p) \right. \\ &\left. \mathbb{E}(\Delta_{g_k}) \right] \left[ \sum_{m=0}^{+\infty} \frac{\beta^m(\phi)}{m!} (-j)^m \mathbb{E}(\mu_k^m) \mathbb{E}(\Delta_{g_k}) \right] \end{aligned} \quad (28)$$

where  $\beta(\phi) = 4\pi(R/\lambda) \sin(\phi/2)$ . On the other hand, we know that

$$J_n(x) = \sum_{p=0}^{+\infty} \frac{(-1)^p}{p!(n+p)!} \left(\frac{x}{2}\right)^{2p+n}, \quad (29)$$

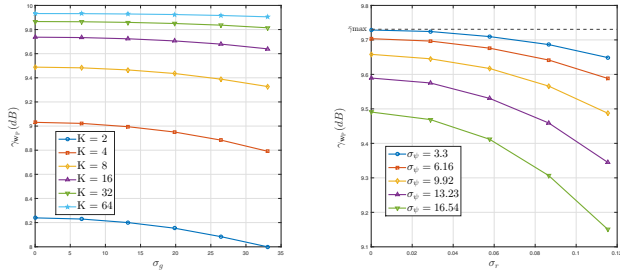
where  $J_n$  stands for the Bessel functions of first kind. Using (29) in (28) leads to

$$\bar{P}_{\tilde{\mathbf{w}}_{\text{opt}}}(\phi) = \frac{1}{K} + \left(1 - \frac{1}{K}\right) \left| \frac{2J_1(\beta(\phi))}{\beta(\phi)} \right|^2 \frac{\sin^2(\sqrt{3}\sigma_g)}{3\sigma_g^2}. \quad (30)$$

It follows from (30) that  $\bar{P}_{\tilde{\mathbf{w}}_{\text{opt}}}(\phi_s = 0) = (1/K) + (1 - (1/K))(\sin^2(\sqrt{3}\sigma_g)/(3\sigma_g^2))$ . Consequently, using  $\tilde{\mathbf{w}}_{\text{opt}}$ , the power received at  $Rx$  decreases with  $\sigma_g$  due to the channel mismatch resulting from implementation errors. This is not surprising since  $\tilde{\mathbf{w}}_{\text{opt}}$  design does not account for such errors. In turn, the average beampattern achieved by the proposed beamformer can be calculated as

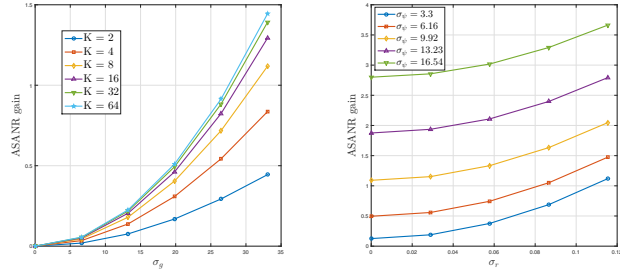
$$\bar{P}_{\mathbf{w}_P}(\phi) = \frac{K + K(K-1) \frac{\sin^2(\sqrt{3}\sigma_g)}{3\sigma_g^2} \left| \frac{2J_1(\beta(\phi))}{\beta(\phi)} \right|^2}{K + K(K-1) \frac{\sin^2(\sqrt{3}\sigma_g)}{3\sigma_g^2}}. \quad (31)$$

The above result verifies that  $\bar{P}_{\mathbf{w}_P}(\phi_s = 0) = 1$  for any given estimation errors. Consequently, the proposed beamformer is much more robust than its conventional counterpart.



(a) ASANR vs. phase jitter and  $K$  (b) ASANR vs. localization and DoA estimation errors

Fig. 2. Proposed robust CB's ASANR in monochromatic environments.



(a) ASANR gain vs. phase jitter and  $K$  (b) ASANR gain vs. localization and DoA estimation errors for  $K = 16$

Fig. 3. Proposed robust CB's ASANR gain in monochromatic environments.

2) *Implementation Option 2*: If Option 2 is adopted, the average beampattern achieved by  $\tilde{\mathbf{w}}_{\text{opt}}$  can be expressed as

$$\begin{aligned} \bar{P}_{\tilde{\mathbf{w}}_{\text{opt}}}(\phi) &= \frac{K}{K^2} + \frac{K(K-1)}{K^2} \sum_{k=1}^K \sum_{l=1, l \neq k}^K \\ &E_{\psi_k} \left\{ e^{-j4\pi R \left[ \mu_k \sin\left(\frac{\phi - \delta\psi_k}{2}\right) - \mu_l \sin\left(\frac{\phi - \delta\psi_l}{2}\right) \right]} \right\} E_{r_k} \left\{ e^{j\frac{2\pi}{\lambda}(\nu_k - \nu_l)} \right\} \\ &= \frac{1}{K} + \left(1 - \frac{1}{K}\right) \xi_r \xi_\psi(\phi). \end{aligned} \quad (32)$$

It follows from (32) that  $\bar{P}_{\tilde{\mathbf{w}}_{\text{opt}}}(\phi_s = 0)$  decreases with  $\sigma_r$  and  $\sigma_\psi$  due to the channel mismatch resulting from implementation errors. In turn, the average beampattern achieved by the proposed beamformer, which accounts for such errors, can be determined as

$$\bar{P}_{\mathbf{w}_P}(\phi) = \frac{K + K(K-1)|\xi_\psi(\phi)\xi_r|^2}{K + K(K-1)|\xi_\psi(0)\xi_r|^2}. \quad (33)$$

It follows from (33) that  $\bar{P}_{\mathbf{w}_P}(0) = 1$  for any localization and DoA estimation errors, in contrast to its conventional counterpart. This validates the robustness of the proposed CB against implementation. Furthermore, from (32) and (33), the proposed robust CB achieves a significant gain over its counterparts in terms of the received desired power. The gain substantially increases with the implementation errors

Now, let us turn our attention to the noise powers. Using  $\tilde{\mathbf{w}}_{\text{opt}}$ , the average noise power can be calculated as

$$\begin{aligned} \bar{P}_{\tilde{\mathbf{w}}_{\text{opt}},n} &= \frac{\sigma_v^2}{K^2} E \left\{ \frac{(\tilde{f}_k - \Delta_{f_k})^H (\tilde{f}_k - \Delta_{f_k})}{|\tilde{f}_k|^2} \right\} + \sigma_n^2 \\ &= \frac{\sigma_v^2(1 + \sigma_f^2)}{K^2} + \sigma_n^2, \end{aligned} \quad (34)$$

In turns,  $\bar{P}_{\mathbf{w}_P,n}$  is given by

$$\bar{P}_{\mathbf{w}_P,n} = \frac{\sigma_v^2(1 + \sigma_f^2)}{K(1 + \sigma_f^2) + K(K-1)\frac{\sin^2(\sqrt{3}\sigma_g)}{3\sigma_g^2}} + \sigma_n^2, \quad (35)$$

if Option 1 is adopted, or

$$\bar{P}_{\mathbf{w}_P,n} = \frac{\sigma_v^2(1 + \sigma_f^2)}{K(1 + \sigma_f^2) + K(K-1)\xi_\psi(0)\xi_r} + \sigma_n^2, \quad (36)$$

if Option 2 is adopted. It could be readily shown from (34)-(36) that  $\bar{P}_{\tilde{\mathbf{w}}_{\text{opt}},n} \geq \bar{P}_{\mathbf{w}_P,n}$ , making  $\bar{\gamma}_{\tilde{\mathbf{w}}_{\text{opt}}} \leq \bar{\gamma}_{\mathbf{w}_P}$  since  $\bar{P}_{\tilde{\mathbf{w}}_{\text{opt}}}(\phi_s) \ll \bar{P}_{\mathbf{w}_P}(\phi)$ .

## V. SIMULATION RESULTS

This section evaluates numerically the performance of the proposed robust CB techniques and compare them with existing CB benchmarks. The empirical quantities are obtained by averaging over  $10^5$  random realizations of  $r_k, \psi_k, [\mathbf{f}]_k$  for  $k = 1, \dots, K$  and  $\alpha_l, \theta_l$  for  $l = 1, \dots, L$ . In all simulations, we assume that the number of rays or chromatics is  $L = 6$ , the noises' powers  $\sigma_n^2$  and  $\sigma_v^2$  are 10 dB below the source transmit power.

Fig. 2 plots the ASANR achieved by the proposed beamformer in monochromatic (i.e., scattering-free) versus the implementation errors' variances  $\sigma^2 = \sigma_g^2 = \sigma_f^2, \sigma_r^2$ , and  $\sigma_\psi^2$  for different values of  $K$ . Fig. 2(a) consider implementation option 1 which results in a phase jitter while Fig. 2(b) consider the implementation option 2 which results in localization and DoA estimation errors. From these figures, the proposed beamformer is able to achieve, even at small  $K$ , optimal performance when the implementation errors are relatively small to moderate (i.e.,  $\sigma^2 \leq 100$  in Option 1 and  $(\sigma_r^2 \leq 4.10^{-4}, \sigma_\psi^2 \leq 10.9)$  in Option 2). This proves the robustness of our proposed CB. For extremely large errors, however, it loses only a fraction of dB. Actually, with the advances made during the two last decades in the field of phase synchronization, localization, and DoA estimation, these implementation errors are often very small, making our beamformer's performance optimal if advanced algorithms are adopted. Nevertheless, the latter naturally come with increased complexity and cost which certainly burden those of WSN nodes. In this context, our proposed beamformer offers the possibility of using inaccurate but low-cost estimation algorithm at negligible performance losses, making it a more practically appealing CB solution. All these observations corroborate the results in Section III.

Fig. 3 displays the proposed CB's achieved ASANR gain against the conventional  $\tilde{\mathbf{w}}_{\text{opt}}$  CB for different  $K$ . Fig. 3(a)

consider the first implementation option while Fig.3(b) consider the second. From these figures, the proposed beamformer largely outperforms its counterpart for any given  $K$ . Indeed, it achieves ASNR gain of 3.7-dB against  $\tilde{\mathbf{w}}_{opt}$ . These gains increase rapidly with both  $K$  and the implementation errors. All these further verify the net superiority of our robust CB technique.

Figs. 4 and 5 show the proposed CB's performance in polychromatic (i.e. scattered) environments. The first plots its achieved ASNR versus implementation errors for different  $K$  while the second plots its ASNR gain against the conventional CB. As expected,  $\mathbf{w}_P$  approaches optimal ASNR performance  $\gamma_{max}$  even in polychromatic environment and this for any  $K$ ,  $\sigma_r^2$ , and  $\sigma_\psi^2$ . In such environment,  $\mathbf{w}_P$  achieves ASNR gain of until 4.3-dB against  $\tilde{\mathbf{w}}_{opt}$ . As can be observed from Fig. 5, these gains rapidly increases with  $K$ ,  $\sigma_r^2$ , and  $\sigma_\psi^2$ . For instance, the ASNR gain over the conventional CB increases by 69.5%, if  $\sigma_r^2$  twice as large. These further verify the high robustness of the proposed CB gainst the implementation impairments.

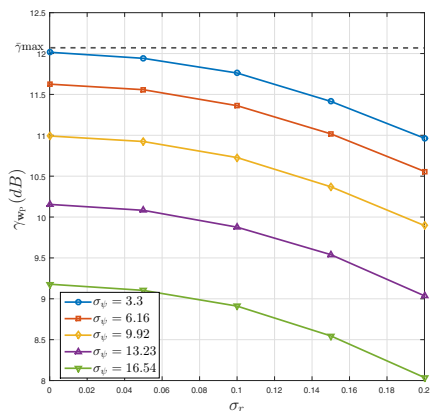


Fig. 4. Proposed robust CB's ASNR vs. localization and DoA estimation errors for  $K = 16$  and  $\sigma_\alpha = 0.115$  in polychromatic environments.

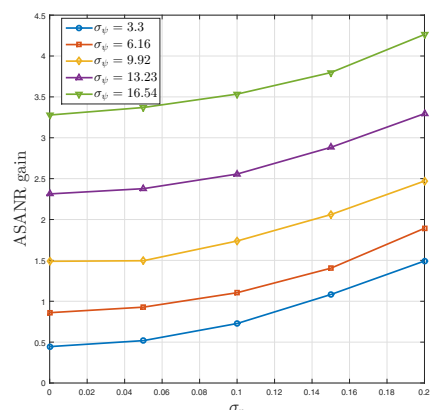


Fig. 5. Proposed robust CB's ASNR gain vs. localization and DoA estimation errors for  $K = 16$  and  $\sigma_\alpha = 0.115$  in polychromatic environments.

## VI. CONCLUSION

We have proposed a new CB solution robust against major implementation impairments over dual-hop transmissions

from a source to a destination communicating through a WSN of  $K$  nodes. Exploiting an efficient asymptotic approximation at large  $K$ , we have developed alternative CB solutions that not only account for estimation errors, but also adapt to different implementation scenarios and wireless propagation environments ranging from monochromatic to polychromatic ones. Besides, in contrast to existing techniques, our new CB solutions are distributed in that they do not require any information exchange among nodes, thereby dramatically improving both WSN spectral and power efficiencies. Simulation results have confirmed that the proposed DCB techniques are much more robust against implementations errors than their benchmarks at much lower complexity.

## REFERENCES

- [1] S. Jayaprakasam, S. K. A. Rahim and C. Y. Leow, "Distributed and Collaborative Beamforming in Wireless Sensor Networks: Classifications, Trends, and Research Directions," *IEEE Communications Surveys & Tutorials*, vol. 19, pp. 2092-2116, June 2017.
- [2] H. Ochiai, P. Mitran, H. V. Poor and V. Tarokh, "Collaborative beamforming for distributed wireless ad hoc sensor networks," *IEEE Trans. Sig. Proc.*, vol. 53, pp. 4110-4124, November 2005.
- [3] M. Bengtsson and B. Ottersten, "Low-complexity estimators for distributed sources," *IEEE Trans. Sig. Proc.*, vol. 48, pp. 2185-2194, August 2000.
- [4] J. Huang, P. Wang and Q. Wan, "Collaborative beamforming for wireless sensor networks with arbitrary distributed sensors," *IEEE Com. Letters*, vol. 16, pp. 1118-1120, July 2012.
- [5] M. F. A. Ahmed and S. A. Vorobyov, "Sidelobe control in collaborative beamforming via node selection," *IEEE Trans. Sig. Proc.*, vol. 58, pp. 6168-6180, December 2010.
- [6] Z. Han and H. V. Poor, "Lifetime improvement in wireless sensor networks via collaborative beamforming and cooperative transmission," *IET microwaves, antennas & propagation*, vol. 1, pp. 1103-1110, December 2007.
- [7] K. Zarifi, A. Ghayeb and S. Affes, "Distributed beamforming for wireless sensor networks with improved graph connectivity and energy efficiency," *IEEE Trans. Sig. Proc.*, vol. 58, pp. 1904-1921, March 2010.
- [8] S. Zaidi and S. Affes, "Distributed Collaborative Beamforming Design for Maximized Throughput in Interfered and Scattered Environments," *IEEE Trans. Comm.*, vol. 63, pp. 4905-4919, October 2015.
- [9] L. C. Godara, "Application of antenna arrays to mobile communications. II. Beam-forming and direction-of-arrival considerations," *IEEE Proc.*, vol. 85, pp. 1195-1245, August 1997.
- [10] B. K. Chalise and L. Vandendorpe, "Optimization of MIMO Relays for Multipoint-to-Multipoint Communications: Nonrobust and Robust Designs," *IEEE Trans. Sig. Proc.*, vol. 58, pp. 6355-6368, July 2009.
- [11] C. G. Tsinos, E. Vlachos, and K. Berberidis, "Distributed blind adaptive computation of beamforming weights for relay networks," *IEEE PIMRC'2013*, London, UK, September 8-11 2013.
- [12] J. Li, A. P. Petropulu, and H. V. Poor, "Cooperative transmission for relay networks based on second-order statistics of channel state information," *IEEE Trans. Sig. Proc.*, vol. 59, no. 3 pp. 1280-1291, March 2011.
- [13] V. H. Nassab, S. Shahbazpanahi, A. Grami, and Z. Q. Luo, "Distributed beamforming for relay networks based on second-order statistics of the channel state information," *IEEE Trans. Sig. Proc.*, vol. 56, no. 9 pp. 4306-4316, September 2008.
- [14] B. Mahboobi, E. Soleimani-Nasab and M. Ardebilipour, "Outage Probability Based Robust Distributed Beam-Forming in Multi-User Cooperative Networks with Imperfect CSI," *Wireless personal communications*, vol. 77, June 2014.
- [15] M. A. M. Sadr, B. Mahboobi, S. Mehrizi, M. A. Attari and M. Ardebilipour, "Stochastic robust collaborative beamforming: non-regenerative relay," *IEEE Trans. Comm.*, vol. 64, pp. 947-958, March 2016.